the Robert A. Welch Foundation (Grant F-126). The calculations were carried out using the CDC 6400/6600 computer at the University of Texas Computation Center. One of us (H.R.) thanks the Science Research Council for the award of a Postdoctoral Fellowship.

References and Notes

(1) Part 33: M. J. S. Dewar, D. Landman, S. H. Suck, and P. K. Weiner, *J. Am. Chem. Soc.*, in press.
(2) M. J. S. Dewar, *Nature (London)*, **176**, 784 (1945); *J. Chem. Soc.*, 406, 707 (1946); "The Electronic Theory of Organic Chemistry", Clarendon Press, Oxford, 1949.
(3) M. J. S. Dewar, *Bull. Soc. Chim. Fr.*, **18**, C71 (1951); *Ann. Rep. Chem. Soc.*, **48**, 112 (1951).
(4) M. J. S. Dewar, *Discuss. Faraday Soc.*, **No. 2**, 50 (1947).
(5) J. Chatt and L. A. Duncanson, *J. Chem. Soc.*, 2939 (1953).
(6) See M. J. S. Dewar and A. P. Marchand, *Annu. Rev. Phys. Chem.*, **16**, 321 (1965).
(7) See G. D. Sargent, "Carbonium Ions", Vol. III, G. A. Olah and P. v. R. Schleyer, Ed., Wiley-Interscience, New York, N.Y., 1972, Chapter 24.
(8) G. A. Olah, G. Liang, G. D. Mateescu, and J. L. Riemensch neider, *J. Am. Chem. Soc.*, **95**, 8698 (1973).
(9) (a) H. C. Brown and K. T. Liu, *J. Am. Chem. Soc.*, **97**, 600, 610 (1975), and papers cited therein; (b) G. Kramer, *Adv. Phys. Org. Chem.*, **11**, 177 (1975).
(10) See M. J. S. Dewar and R. C. Dougherty, "The PMO Theory of Organic Chemistry", Plenum Press, New York, N.Y., 1975.
(11) For objections to the use of the Hückel method in this connection, see C. A. Coulson and M. J. S. Dewar, *Discuss. Faraday Soc.*, **No. 2**, 54 (1947).
(12) R. C. Bingham, M. J. S. Dewar, and D. H. Lo, *J. Am. Chem. Soc.* **97**, 1285 (1975).
(13) J. L. Franklin, J. G. Dillard, H. M. Rosenstock, J. J. Herron, K. Draxl, and F. H. Field, "Ionization Potentials, Appearance Potentials, and Heats of Formation of Gaseous Positive Ions", National Bureau of Standards, Washington, D.C., 1969.
(14) S. L. Chong and J. L. Franklin, *J. Am. Chem. Soc.*, **94**, 6347 (1972).
(15) (a) C. C. J. Roothaan, *Rev. Mod. Phys.*, **23**, 69 (1951); (b) G. G. Hall, *Proc. R. Soc. London, Ser. A*, **205**, 541 (1951).
(16) P. C. Hariharan, L. Radom, J. A. Pople, and P. v. R. Schleyer, *J. Am. Chem. Soc.*, **96**, 599 (1974).
(17) R. C. Bingham, M. J. S. Dewar, and D. H. Lo, *J. Am. Chem. Soc.*, **97**, 1294, 1302, 1307 (1975).
(18) M. J. S. Dewar and R. C. Haddon, *J. Am. Chem. Soc.*, **97**, 2278 (1975).
(19) W. J. Hehre, R. F. Stewart, and J. A. Pople, *J. Chem. Phys.*, **51**, 2657 (1969).
(20) J. W. McIver, Jr., and A. Komornicki, *Chem. Phys. Lett.*, **10**, 303 (1971).
(21) B. A. Murtagh and R. W. H. Sargent, *Comput. J.*, **13**, 185 (1970).
(22) See M. J. S. Dewar and S. Kirschner, *J. Am. Chem. Soc.*, **93**, 4290 (1971).
(23) J. W. McIver, Jr., and A. Komornicki, *J. Am. Chem. Soc.*, **94**, 2625 (1972).
(24) P. v. R. Schleyer, W. E. Watts, R. C. Fort, Jr., M. B. Comisarov, and G. A. Olah, *J. Am. Chem. Soc.*, **86**, 5679 (1964).
(25) M. Saunders, P. v. R. Schleyer, an l G. A. Olah, *J. Am. Chem. Soc.*, **86**, 5680 (1964).
(26) H. C. Brown, *Acc. Chem. Res.*, **6**, 377 (1973).
(27) M. J. S. Dewar, "The Molecular Orbital Theory of Organic Chemistry", McGraw-Hill, New York, N.Y., 1969.
(28) J. A. J. Jarvis, B. T. Kolbourn, and P. G. Owston, *Acta Crystallogr., Sect. B*, **27**, 366 (1971).
(29) MINDO/3 calculations[30] indicate that the ^{13}C NMR spectra of **2**, and of a rapidly equilibriating mixture of classical ions (**1** $\rightleftarrows$ **6**), would be almost identical. While MINDO/3 calculations of ^{13}C NMR parameters are by no means perfect, the comparison of **2** with (**1** $\rightleftarrows$ **6**) should be significant. The values calculated for **2** in fact agree well with experiment, somewhat better than those for (**1** $\rightleftarrows$ **6**).
(30) M. J. S. Dewar and D. Landman, in press.
(31) G. A. Olah, G. D. Mateescu, and J. L. Riemenschneider, *J. Am. Chem. Soc.*, **94**, 2529 (1972).
(32) G. A. Olah and G. Liang, *J. Am. Chem. Soc.*, **95**, 3792 (1973).
(33) G. Sebold, P. Vogel, M. Saunders, and K. B. Wiberg, *J. Am. Chem. Soc.*, **95**, 2045 (1973).
(34) R. Ditchfield, W. J. Hehre, and J. A. Pople, *J. Chem. Phys.*, **54**, 724 (1971).
(35) RH calculations, using the STO-3G and 4-31G basis sets, gave much too high an energy for the pyramidal nonclassical $(CH)_5^+$ ion.[36] The MINDO/3 results[37] were much more reasonable.
(36) W. J. Hehre and P. v. R. Schleyer, *J. Am. Chem. Soc.*, **95**, 5837 (1973).
(37) M. J. S. Dewar and R. C. Haddon, *J. Am. Chem. Soc.*, **95**, 5836 (1973).
(38) K. Siegbahn et al., *Nova Acta Regiae Soc. Sci. Ups.*, **20**, 1 (1967).
(39) M. J. S. Dewar and D. H. Lo, *Chem. Phys. Lett.*, **33**, 298 (1975).
(40) W. L. Jolly, *J. Am. Chem. Soc.*, **92**, 3260 (1970).
(41) G. A. Olah, G. D. Mateescu, L. A. Wilson, and M. H. Gross, *J. Am. Chem. Soc.* **92**, 7231 (1970).
(42) M. J. S. Dewar, S. H. Suck, and P. K. Weiner, *Chem. Phys. Lett.*, **29**, 220 (1974).
(43) P. E. Rusch, Ph.D. Dissertation, University of Texas at Austin, 1971.
(44) Deconvolution of spectra should, in our opinion, always be carried out by digitization and computer analysis rather than by the use of curve analyses. The results given by the latter tend to be too subjective and one has no indication of the statistical probability of the fit.
(45) G. Olah, *Acc. Chem. Res.*, **9**, 41 (1976).

A Derivation of the Shapes and Energies of the Molecular Orbitals of 1,3-Dipoles. Geometry Optimizations of These Species by MINDO/2 and MINDO/3

Pierluigi Caramella,[1a] Ruth Wells Gandour, Janet A. Hall, Cynthia Gray Deville, and K. N. Houk*[1b]

Contribution from the Department of Chemistry, Louisiana State University, Baton Rouge, Louisiana 70803. *Received March 3, 1976*

Abstract: The energies and shapes of the frontier molecular orbitals of 1,3-dipoles determine the reactivities and regioselectivities of these species. The reasons that the frontier molecular orbitals of 1,3-dipoles have the shapes and energies they do are deduced here by qualitative perturbation theory. MINDO/2 and MINDO/3 calculations on all the parent 1,3-dipoles have been performed with geometries optimized by the procedure of McIver and Komornicki for MINDO/2 and by the procedure of Dewar for MINDO/3. The geometrical trends observed for the nitrilium betaines deviate significantly from those commonly assumed, but fit experimental data for HCNO, and ab initio STO-3G calculations on these systems. The resulting Koopmans' theorem ionization potentials and electron affinities from MINDO/2 are in close agreement with our earlier empirical estimates, and indicate the suitability of MINDO/2 for calculation of ionization potentials and electron affinities of these systems.

The rates and regioselectivities of reactions of 1,3-dipoles with alkenes and alkynes have been studied experimentally for many years,[2] but a theoretical framework for the understanding of these reactions was developed only recently.[3-6] In spite of the simplicity of the frontier molecular orbital treatment of these reactions, the understanding of why the method works is truly attainable only after it is understood why the frontier molecular orbitals of 1,3-dipoles and dipolarophiles

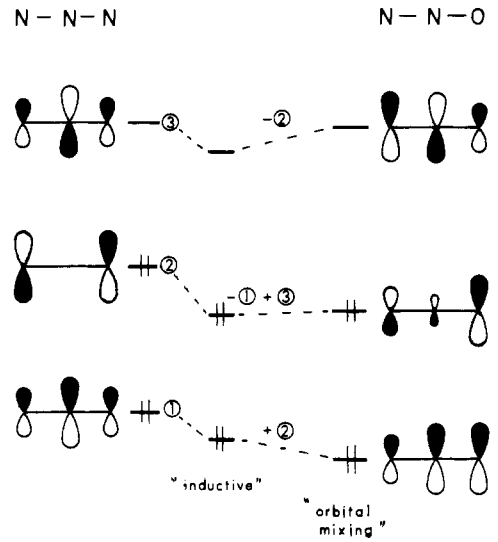

Figure 1. Perturbation analysis of the conversion of the π system of azide ion to that of nitrous oxide.

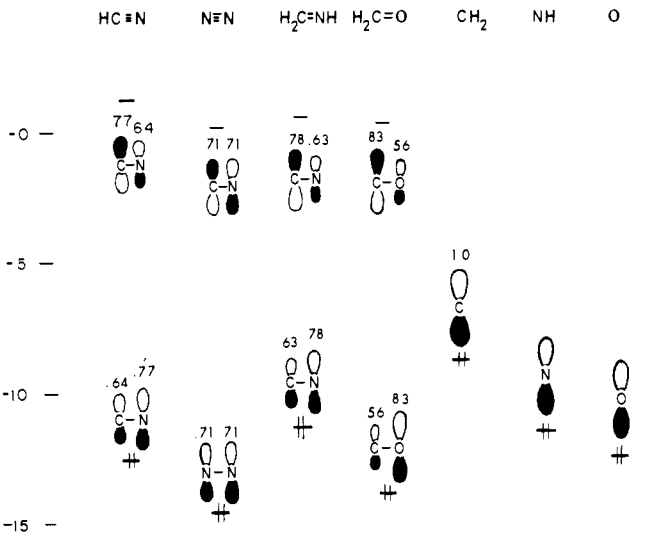

Figure 2. π MO energies of the 1,3-dipole fragments.

have the shapes and energies that result from quantum mechanical calculations on these systems. In this paper we show how the frontier molecular orbitals of the dipoles can be built up from the fragments using perturbation theory. The relative influence of inductive and conjugative effects is evaluated using MINDO/2 calculations with successive deletion of various matrix elements.

Geometry optimizations by MINDO/2 and MINDO/3 for the parent dipoles show slight deviations from planarity for several dipoles. Nitrile ylides are, however, predicted to be highly bent, and the bent form of nitrile imines is comparable in stability to the planar form. The reasons for the bending are discussed and the geometries are compared with the ab initio STO-3G calculations we have reported elsewhere.

Although it is known that calculations neglecting differential overlap exhibit some deficiencies in treatment of molecules containing lone pairs on adjacent atoms, MINDO/2 calculations yield surprisingly good ionization potentials and electron affinities without further empirical correction. Not surprisingly, the geometries obtained by MINDO/3 are somewhat better, but the IP's and EA's are worse than those obtained by MINDO/2.

Qualitative Derivations of the Shapes of 1,3-Dipole Molecular Orbitals

The common 1,3-dipoles, X-Y-Z, have a 4π-electron system, isoelectronic with the allyl anion system. One procedure for deriving the shapes of the three π orbitals which result from mixing of three basis 2p orbitals is to begin with the familiar allyl orbitals and to consider, by perturbation methods,[10] the effects of altering the electronegativity (or basis orbital energy) of one or several of the component atoms and altering the resonance integrals due to bond length changes and the type of atoms involved.

For example, Figure 1 shows the formal conversion of one π system of the azide ion to that of nitrous oxide. The familiar π orbitals of a symmetric three orbital array are shown at the left. Substitution of oxygen for one nitrogen atom terminus will result in a first-order lowering of the energy of all the π orbitals and the removal of orthogonality between the various π orbitals. As a result, mixing of the various orbitals will occur to give the final nitrous oxide orbitals. That is, each of the azide orbitals, ψ_1, ψ_2, and ψ_3, will be perturbed by mixing with the others to give a new set of orbitals, ψ_i'. For example,

$$\psi_1' = N[\psi_1 + \Sigma_i C_{1i}\psi_i]$$

where ψ_1' is the perturbed orbital arising from mixture of ψ_2 and ψ_3 with ψ_1, N is the normalization factor, and the C's are mixing coefficients which can be obtained from standard second-order perturbation theory.[10,11] To calculate the extent of mixing of ψ_j into ψ_i,

$$C_{ij} = \frac{\langle \psi_i | h | \psi_j \rangle}{\epsilon_i - \epsilon_j}$$

where h is the perturbation, which, in this case, is the increase in electronegativity of a terminal atom. This perturbation causes the numerator of the expression given above to have a negative sign, as long as the coefficients at the site of perturbation (one N terminus) are taken to be of the same sign in ψ_i and ψ_j. When ϵ_i is less than ϵ_j, C_{ij} will be positive. In general, a lower energy orbital will mix in higher energy orbitals "in phase" at the site of perturbation, and higher energy orbitals will mix in lower energy orbitals "out-of-phase" at the site of the perturbation.

In the case under consideration, the MINDO/2 orbitals of nitrous oxide (reported later) can be shown to be the following linear combination of azide orbitals:

$$\psi_1' = 0.99\psi_1 + 0.05\psi_2 + 0.05\psi_3$$
$$\psi_2' = 0.98\psi_2 - 0.06\psi_1 + 0.16\psi_3$$
$$\psi_3' = 0.98\psi_3 - 0.16\psi_2 - 0.03\psi_1$$

While this method can rationalize shapes and energies of 1,3-dipole molecular orbitals, an alternative, more readily applied, and considerably more revealing method consists of the formal union of the π systems of a diatomic fragment, X-Y, with the lone pair of a monatomic fragment, Z.

For the common parent 1,3-dipoles, the heavy atoms of the XY fragments are CN, CO, OO, and NN. In the 1,3-dipoles "with a double bond", the molecules containing the appropriate π systems are HCN, singlet O_2, and N_2, while for the 1,3-dipoles "without a double bond", the appropriate model XY molecules are H_2CNH and H_2CO. The appropriate Z fragments in both types of molecules are singlet states of CH_2, NH, and O. The relative energies and shapes of the molecular orbitals of these fragments, obtained by MINDO/2, are shown in Figure 2.

The formation of the σ bond between the XY and the 2 fragment formally involves an in-plane lone-pair orbital on atom Y and a vacant orbital on the Z fragment. Through this union, Y acquires a formal positive charge, increasing the effective electronegativity of this atom, while Z acquires a negative charge, decreasing its effective electronegativity. This

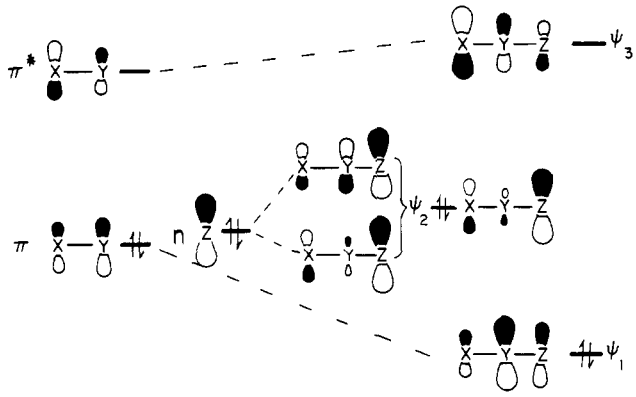

Figure 3. Qualitative derivations of the π MO's of a 1,3-dipole consisting of electropositive XY and relatively electronegative Z fragments.

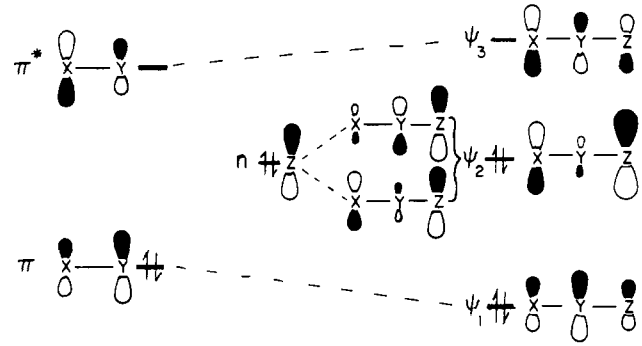

Figure 4. Qualitative derivations of the π MO's of a 1,3-dipole consisting of electronegative XY and relatively electropositive Z fragments.

has the consequence of lowering the XY π orbital energies and of raising the π orbital energy of Z.[8] A further consequence is the distortion of the π and π^* orbitals of the X-Y fragment toward Y in π and toward X in π^* as Y becomes more electronegative. This results from the type of mixing of the π and π^* orbitals discussed earlier. That is, the π orbital will mix in some of the π^* "in-phase" at the site of increased electronegativity, while π^* mixes in some of the π "out-of-phase" at this site. The CN and CO fragments become more polarized and the originally symmetrical NN and OO fragments acquire polarization in this way.

Using the orbital energies in Figure 2, the shapes and energies of π MO's for planar arrangements of the dipoles can be qualitatively derived. Both bond length and angle changes occur upon union of the fragments, but the orbital shapes remain essentially those derivable by a direct union of isolated fragments.

We consider two extremes. In Figure 3, we show the union of a relatively electropositive XY (fragment (e.g., HCN) with a relatively electronegative Z fragment (e.g., O). The filled and vacant π orbitals of the XY fragment are designated "π" and "π^*", respectively, while the π orbital of the Z fragment is designated "n". Upon σ formation between fragments, π and π^* will be stabilized and n will be destabilized due to the electronegativity changes outlined above. The consequences of mixing of the π, π^*, and n orbitals can be deduced by the usual rules of orbital mixing:[10,11] those orbitals closest in energy will mix most; a given orbital will mix with a higher energy orbital in a bonding fashion to produce a lower energy orbital, and in an antibonding fashion to produce an orbital which is higher in energy than either of the starting orbitals. In a treatment of the union of a two orbital system (π and π^*) with a single orbital system (n), the final shape of the n orbital will be an additive result of individual perturbations by the π and π^* orbitals.

The lowest π orbital (ψ_1) of the composite 1,3-dipole π system is the π mixed in a bonding fashion with n, and the LUMO of the 1,3-dipole is mainly the XY π^* orbital, which has mixed slightly with the n orbital of Z in an antibonding fashion. The HOMO of XYZ is a mixture of all three orbitals but, in this case, results mainly from the antibonding admixture of the n orbital of Z with the close energy XY π orbital. This admixture gives a much larger coefficient at Z than at X and a node between Y an Z. These coefficient magnitudes result both because ψ_2 has more "n" than "π" character and because the "π" orbital mixed in has a smaller coefficient at X than at Y. The trends in coefficient sizes are moderated somewhat by the in-phase admixture with the π^* orbital which has a larger coefficient at X than at Y. The more the π^* orbital mixes with n, the smaller the ratio of Z to X coefficients becomes. The central Y coefficient also diminishes and eventually the node may appear between X and Y, if π^* admixture is sufficiently large.

These trends are shown in Figure 4, where the Z fragment has been made relatively electropositive with respect to the XY fragment. In the LUMO, the X coefficient is still larger than that at Z, but the difference is smaller than for Figure 3. Similarly, the terminal coefficients in ψ_2 are more equal, and the central coefficient has nearly vanished. These qualitative diagrams explain the trends noted in our earlier calculations on all of the parent 1,3-dipoles by CNDO/2 methods.[5] That is, as one proceeds along any of the series from ylide to oxide, the HOMO and LUMO energies decrease regularly. In all species, the larger HOMO terminal coefficient is on Z (CH_2, NH, or O). From the constructions in Figures 3 and 4, this can be seen to result from the fact that all the HOMO's are more like the Z lone pair fragment in composition. As the electronegativity of the Z fragment is increased from CH_2 to NH to O, the difference in HOMO terminal coefficient magnitudes increases, essentially a result of the increasing admixture of n with a π orbital that has a small X coefficient and decreasing admixture with a π^* orbital that has a large X coefficient.

The LUMO trends are also readily explained. As the Z electronegativity increases, less admixture of the π_{XY}^* orbital with the Z fragment occurs, and the orbital becomes more purely π_{XY}^* in nature. In all cases, however, the LUMO of the 1,3-dipole is most properly identified with a π_{XY} orbital of the XY fragments.

The nucleophilicity of a molecule will increase as the energy of the HOMO increases, while the nucleophilicity at a particular atom in the molecule will increase as the HOMO coefficient at the atom increases. Since the HOMO energy along a given XYZ series increases as Z changes from O to NH to CH_2, the gross nucleophilic reactivity of dipoles should increase along this series. The differentation between the nucleophilicities of the X and Z termini increases in the opposite order, however. That is, if X and Z are of similar electronegativity, the HOMO coefficient at Z makes Z only slightly more nucleophilic than the X terminus. However, as Z is made more electronegative, the Z coefficient in the HOMO increases at the expense of the X coefficient. The negative charges behave similarly; as the electronegativity of Z increases, the extent of negative charge at Z increases at the expense of that at X. Thus, in nitrile ylides, the nucleophilicities of the two terminal carbons are expected to be nearly identical, while in nitrile oxide, the oxygen is much more nucleophilic than carbon even though a nitrile oxide is overall less nucleophilic than nitrile ylide. Although we do not wish to deal at length with these trends at this time, it may be of interest to note that the oxygen of nitrous oxide is a "hard" nucleophilic site, while both carbons of nitrile ylides are "soft" nucleophilic sites. Similar trends can be noted for the other 1,3-dipole series.

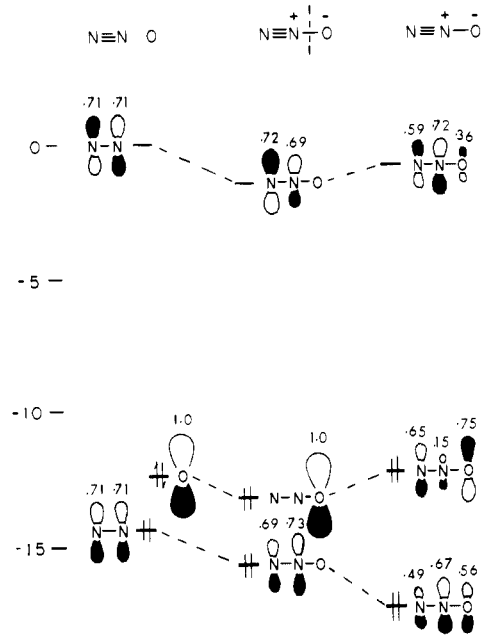

Figure 5. MINDO/2 π orbitals for (a) N_2 and O, (b) N_2O with one N-O π interaction deleted, and (c) N_2O.

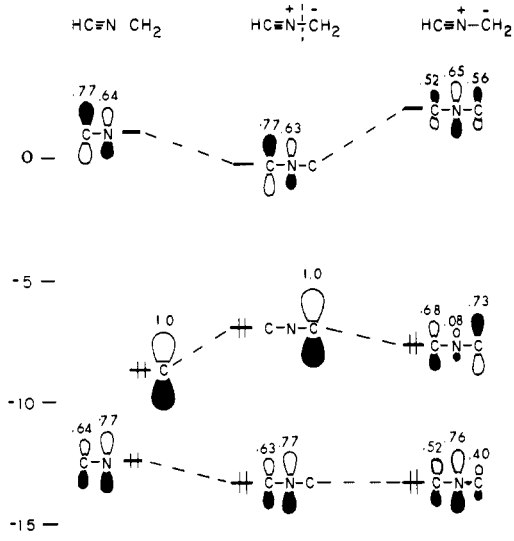

Figure 6. MINDO/2 construction of the π orbitals of formonitrile ylide.

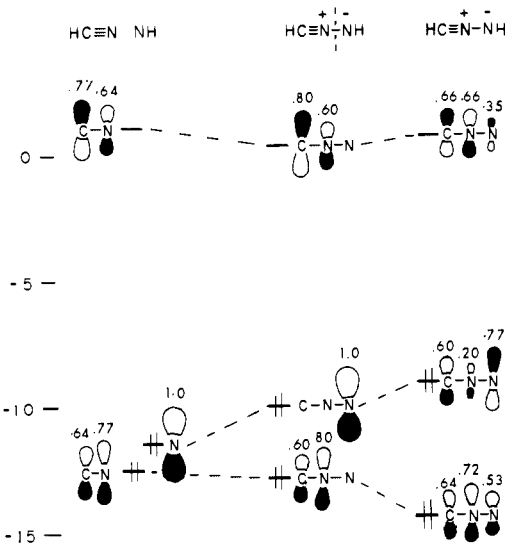

Figure 7. MINDO/2 construction of the π orbitals of formonitrile imine.

The electrophilicity orders are more easily identified. Changing the Z moiety from CH_2 to NH to O will result in increase in electrophilicity of the 1,3-dipole, primarily at the X terminus. That is, progressing along this series, the LUMO energy drops, the LUMO coefficient at X increases, and the positive charge at X decreases. All these effects work in harmony to increase electrophilicity, particularly at the X terminus. The 1,3-dipole π MO's calculated by CNDO/2,[5] MINDO/2, and MINDO/3 (reported in the next section), or ab initio techniques give remarkably detailed agreement with the qualitative considerations given above. This depends on the fact that our qualitative derivation started from the fragments which more nearly retain their identities in the 1,3-dipoles. For example, the N_x-N_y bond length in diazoalkanes and azides (1.12 Å) is only slightly longer than the NN bond length of nitrogen (1.10 Å). Another way of saying this is that the valence-bond structures, $X{\equiv}Y^+{-}Z{:}^-$ or $X{=}Y^+{-}Z{:}^-$, are somewhat closer to the electronic structures of the 1,3-dipoles than the other all-octet valence-bond structures, $:X^-{=}Y^+{=}Z$ or $:X^-{-}Y^+{=}Z$. However, the latter may gain in importance as X and Z become more nearly equal in electronegativity, resulting in remarkable geometry changes away from planarity, as discussed below.

Computational Verifications of the Qualitative Derivations of Orbital Shapes

The qualitative analysis presented in the previous section is supported by the stepwise constructions of several of the 1,3-dipoles, using the MINDO/2 method. Figure 5 shows the π orbital energies calculated for the nitrogen molecule and an oxygen atom in a singlet state. This case is similar to the one shown in Figure 3. As suggested in the preceding section, union of N_2 with O, without allowing the π_z interaction between the central N $2p_z$ and O $2p_z$ orbitals,[12] results in both a decrease in energy of the nitrogen π orbitals and the polarization discussed previously. In this calculation, the central N bears a total charge of +0.08, and the terminal N and O atoms have charges of −0.28 and −0.53, respectively. Thus, the π interaction involving the $2p_y$ orbitals and the σ interaction has already allowed considerable transfer of charge from oxygen onto the N_2 fragment.

Upon including the matrix element for interaction of the $2p_z$ orbitals of the central N and the O atoms, the expected lowering of the π orbital to give the ψ_1 and increase of the π^* orbital to give ψ_3 occurs. The energy of ψ_2 is raised from that of the n due to the greater mixing with π than with the π^* orbital of the N_2 fragment. Conjugation further decreases the negative charge on O and increases the negative charge on the terminal nitrogen. In Figures 6-8, similar stepwise constructions of the π orbitals of planar or linear nitrilium betaines are shown. In each of these calculations, the trends deduced in Figures 3 and 4 are verified. Union of the nitrile π orbitals and an excited singlet methylene fragment (of $a_1^0b_1^2$ configuration; the energies were estimated by carrying out a calculation of a linear singlet) without π interaction (the z-z π matrix element was deleted) gives the expected stabilization of the π_{CN} and π^*_{CN} orbitals and destabilization of the n_{CH_2} orbital. The π orbitals have slightly increased polarization. Finally, including the π interaction leads to orbital energy changes qualitatively like those in Figure 4. Since we are using an SCF method, reorganization of charge results in changes in diagonal matrix elements, or effective electronegativities, of component atoms, and orbital energy changes are not as simple as Figures 3 and 4 would indicate. Second, our previous analysis has neglected

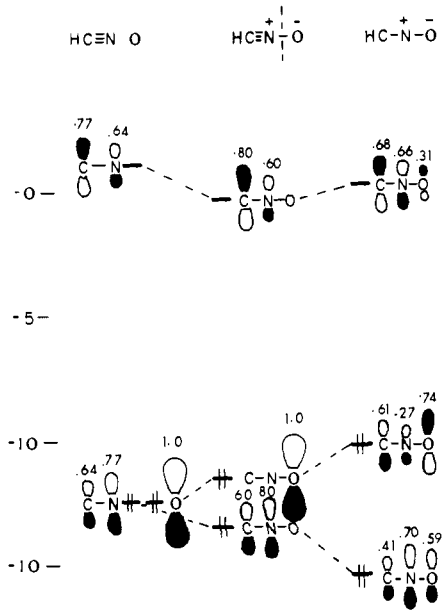

Figure 8. MINDO/2 construction of the π orbitals of formonitrile oxide.

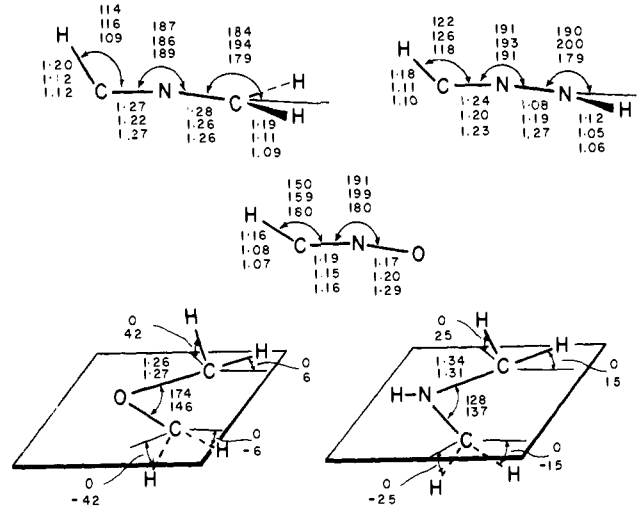

Figure 9. Geometries of nonplanar 1,3-dipoles. Angles and bond lengths (Å) listed are (top to bottom): MINDO/2, MINDO/3, STO-3G.[13]

the second-order π, π^* mixing which additionally alters the shapes of ψ_1, ψ_2, and ψ_3. Nevertheless, the frontier orbital energy changes and shapes were predicted rather well by the simplified analysis. The n_{CH_2} orbital is stabilized due to greater interaction of this orbital with the π^*_{CN} orbital than with the π_{CN} orbital. The change in position of the node in the HOMO and the nearly identical terminal coefficients in the LUMO are indicative of this substantial interaction.

Turning to the nitrile imine construction (Figure 7), the qualitative trends expected when the π_{CN} and n_- fragments are closer in energy are observed. The trend is further enforced in the nitrile oxide (Figure 8). As the n-π_{CN} interaction becomes dominant, the central coefficient in the HOMO increases, the ratio of magnitudes of the O to C coefficient increases in the HOMO, and the LUMO becomes more purely π^*_{CN} in nature.

MINDO/2 and MINDO/3 Optimized Geometries

The OPTMO program of Komornicki and McIver, which incorporates MINDO/2 energy and gradient calculations,[7] and the MINDO/3 program, which uses Dewar's new parametrization and a similar (Davidon-Fletcher-Powell) gradient technique for location of minima, were used to find the optimum geometries of the simple 1,3-dipoles. The optimized geometrical parameters of the dipoles obtained by both techniques are shown in Table I. Although many of the dipoles have planar or quasi-planar geometries, as is usually assumed, significant deviations from planarity are found for the nitrilium betaines and for azomethine and carbonyl ylides. The geometries of these nonplanar dipoles are more clearly displayed in Figure 9.

As pointed out by Dewar and others,[9] MINDO and other ZDO methods treat molecules with a lone pair on adjacent atoms relatively poorly. The optimized geometries of the dipoles however, compare very well with the available experimental geometries given in Table I and with the ab initio geometries of nitrilium betaines,[13] which are given for comparison in Figure 9.

Nitrile ylide appears to be definitely bent with an HCN angle of 114–116°. The stabilization over the optimized planar form also shown in Figure 9 is calculated to be 12.9 (MINDO/2) and 16.4 kcal/mol (MINDO/3). These figures compare well with the 11.1 (4-31G) and 22.4 kcal/mol (STO-3G) found in the ab initio optimization.[9,18]

Nitrile imine is also predicted to be bent with an HCN angle ranging from 122° (MINDO/2) to 126° (MINDO/3). The preference over the planar is, however, only slight: 2.2 kcal/mol in MINDO/2, and 3.2 kcal/mol in MINDO/3. Ab initio calculations also predict similar stabilities for the two forms, the bent being favored by 2.2 kcal/mol at the STO-3G level and the planar being favored by 3.9 kcal/mol at the 4-31G level.[18]

Nitrile oxide is nonlinear both in MINDO/2 and in MINDO/3 optimizations. The linear form is 0.2 (MINDO/2) and 0.11 kcal/mol (MINDO/3) more stable than the bent. This compares astonishingly well with the available microwave and far ir data on fulminic acid.[14] The STO-3G geometrical search failed to reproduce the experimental hump; the linear geometry is favored both at the STO-3G and 4-31G levels.[18]

By contrast, diazonium betaines are substantially planar. In the case of hydrazoic acid, both types of calculations give a slight deviation from linearity for the NNN moiety with the hydrogen bent out of the plane defined by the three nitrogens.

For the "allyl type" 1,3-dipoles, the drawings at the bottom of Figure 9 define the type of nonplanarity observed. The angle θ given there and in Table I is that angle between the plane of the heavy atoms and the bond to hydrogen and is taken as positive for hydrogens above the plane and negative for hydrogens below the plane. This angle is reproducible to within ±2°, depending on the starting geometry used in the optimization. The azomethine ylide and carbonyl ylide are nearly planar in MINDO/2 but are significantly pyramidalized at the CH_2 groups in MINDO/3. However, the energetic preference of MINDO/3 for the nonplanar form is only slight for the azomethine ylide (2.6 kcal/mol) but is considerably larger for the carbonyl ylide (17.2 kcal/mol). MINDO/3 has been parametrized in such a way that water is bent and ammonia is nonplanar (in contrast to MINDO/2) so that inversion barriers are treated more realistically, and the calculated nonplanarity in MINDO/3 is likely real.[19]

Parenthetically, allyl anion is planar in MINDO/3, so a trend of increasing nonplanarity is observed as one proceeds along the isoelectronic series >C-H(-), >N-H, >O. Further studies are in progress to determine the origin of this effect, as well as to determine changes in geometries which may result from taking configuration interaction into account. The latter may be necessary since these molecules have appreciable di-

Table I. MINDO/2 and (MINDO/3) Calculated and [Experimental] Geometries of 1,3-Dipoles[a]

H—C≡N⁺—Z⁻(H)

E_{rel}	Z(H)	r_{HC}	r_{CN}	r_{NZ}	r_{ZH}	∠HCN	∠CNZ	∠HCNZ	∠NZH	∠CNZH	ϕ[h]
0.0	CH_2	1.20 (1.12)	1.27 (1.22)	1.28 (1.26)	1.19 (1.11)	114 (116)	173 (174)	180 (180)	120 (123)	88 (81)	184 (194)
+12.9 (16.4)	CH_2 (planar)	1.15 (1.07)	1.27 (1.17)	1.31 (1.28)	1.118 (1.10)	180 (180)	180 (180)	(–)	118 (121)	(–)	180 (180)
0.0	NH	1.18 (1.11)	1.24 (1.20)	1.08 (1.19)	1.12 (1.05)	122 (126)	169 (167)	154 (141)	124 (115)	109 (120)	190 (200)
+2.2 (3.2)	NH (planar)	1.16 (1.08)	1.20 (1.17)	1.10 (1.20)	1.11 (1.04)	152 (159)	176 (177)	(–)	123 (116)	(–)	180 (180)
0.0	O	1.16 (1.08) [1.06][b]	1.19 (1.15) [1.16][b]	1.17 (1.20) [1.21][b]		150 (159) [161][b]	169 (171) [180][b]	(–)			
+0.2 (0.11)	O (linear)	1.15 (1.07)	1.18 (1.15)	1.18 (1.20)		180 (180)	180 (180)				

N≡N⁺—Z⁻(H)

Z(H)	r_{NN}	r_{N-Z}	r_{Z-H}	∠NNX	∠NZH	θ[i]
CH_2	1.03 (1.11) [1.12][d]	1.30 (1.27) [1.32][d]	1.18 (1.10) [1.08][d]	180 (180) [180]	118 (125) [117]	0 (0)
NH	1.01 (1.11) [1.13][e]	1.06 (1.19) [1.29][e]	1.11 (1.03) [0.98][e]	173 (168) [180][e]	132 (119) [114][e]	14 (0) [0]
O	1.01 (1.09) [1.13][f]	1.15 (1.20) [1.19][f]		180 (180) [180]		

$H_2C{=}N^+{-}Z^-(H)$ (H on N)

Z(H)	r_{HC}	r_{CN}	r_{NZ}	r_{NH}	r_{ZH}	∠HCN[c]	∠CNZ	∠NZH[c]	θ[c,i]
CH_2	1.19 (1.10)	1.34 (1.31)	1.34 (1.31)	1.13 (1.05)	1.19 (1.10)	1.19, 119 (119, 119)	128 (137)	119, 119, (119, 119)	0 (15, 25, –15, –25)
NH	1.19 (1.10)	1.32 (1.29)	1.14 (1.24)	1.14 (1.05)	1.13 (1.05)	119, 121 (123, 124)	118 (141)		0 (0)
O	1.19 (1.10)	1.32 (1.27)	1.22 (1.23)	1.15 (1.06)		124, 119 (123, 123)	126 (133)		0 (0)

$H_2C{=}O^+{-}Z^-(H)$

Z(H)	r_{HC}	r_{CO}	r_{OZ}	r_{ZH}	∠HCO[c]	∠COZ	∠OZH[b]	θ[c,i]
CH_2	1.20 (1.10)	1.26 (1.27)	1.26 (1.27)	1.20 (1.10)	123, 123 (122, 115)	174 (146)	123, 123 (122, 115)	0 (6, 42, –6, –42)
NH	1.21 (1.11)	1.24 (1.22)	1.22 (1.30)	1.14 (1.06)	125, 123 (127, 119)	162 (144)	121 (115)	0 (0)
O	1.21 (1.11)	1.24 (1.23)	1.21 (1.30)		124, 124 (129, 116)	180 (126)		0 (0)

Ozone

r_{OO}	∠OOO
1.20 (1.25) [1.278]	148 (126) [116.75][g]

[a] Bond lengths in Å; angles in deg. Experimental geometries are given in brackets. [b] B. P. Winnewisser, M. Winnewisser, and F. Winther, *J. Mol. Spectrosc.*, 51, 65 (1974). [c] Inner hydrogen angle listed first. [d] A. P. Cox, L. F. Thomas, and J. Sheridan, *Nature (London)*, 181, 1000 (1958). [e] J. L. Griggs, Jr., K. N. Rao, L. H. Jones, and R.M. Potter, *J. Mol. Spectrosc.*, 25, 34 (1968). [f] M. Winnewisser and R. L. Cook, *J. Chem. Phys.*, 41, 999 (1964). [g] R. H. Hughes, *ibid.*, 24, 131 (1956). [h] ϕ = angle between N–Z bonds and a line (shown in Figure 9) formed by the intersection of the CNZ and the NZH planes. [i] θ = angle between CXZ plane and the XH bond (shown for the bottom two drawings in Figure 9).

radical character.[14] As can be seen from Figure 9, both the carbonyl ylide and azomethine ylide are not only pyramidalized at the methylene groups, but the terminal methylenes have been rotated in a conrotatory fashion away from planarity (or, alternatively, from the oxirane and aziridine geometrical minima). This type of distortion is experimentally observed in stabilized thiocarbonyl ylides and is exaggerated by MINDO/3 calculations for these push-pull stabilized species.[15]

MINDO/3 is significantly better than MINDO/2 at reproducing the experimental geometries known for some 1,3-dipoles. The comparison with the STO-3G optimized nitrilium betaine geometries of Figure 9 is also reasonable. A maximal difference in bond lengths of about 0.1 Å occurs at the CN of the bent ylide and at the N–N and N–O bonds of the imine and oxide. This is consistent with the expectation that MINDO does not properly treat adjacent lone pair interactions.

Another noteworthy feature of the MINDO geometries is the arrangement of substituents at the termini of the dipoles. For the bent nitrilium ylide and imine, the CH_2 and NH bonds bend "inside", whereas ab initio gives a small but definite "outside" bending. Similarly in the planar imine, the HCN bending accompanying the dominating NNH bending occurs inside; ab initio calculations again give a preference for the outside bending of HCN. The same trends are found in the other dipoles and, somewhat magnified, in the azomethine and carbonyl ylides.

The preference for HCN bending with decreasing electronegativity of the Z terminus can be qualitatively understood in valence bond (VB) terminology. Where Z is more electronegative than X, the charge and the HOMO density localized at the Z terminus so that the VB structure, $X{\equiv}Y^+{-}Z^-$, represents the electronic structure of the dipole fairly well. The formal negative charge at Z can be stabilized by bending at Z, which mixes in s character. The planar nitrile imine shows the expected bending at N_3. When Z is of comparable elec-

Table II. A Comparison of the Measured or Estimated IP's and EA's of 1,3-Dipoles and the Negatives of MINDO/2 and MINDO/3 HOMO and LUMO Energies (in eV)

Dipole	IP[a]	MINDO/2 $-\epsilon$(HOMO)	MINDO/3 $-\epsilon$(HOMO)	EA	MINDO/2 $-\epsilon$(LUMO)	MINDO/3 $-\epsilon$(LUMO)
$HCNCH_2$	7.7	8.58	8.30	−0.9	−0.42	−1.38
HCNNH	9.2	9.32	8.59	−0.1	−0.18	−1.27
HCNO	*10.8*[b]	10.34	10.22	0.5	0.30	−0.99
$NNCH_2$	*9.0*	9.06	7.99	−1.8	−0.20	−1.58
NNNH	*10.7*[c]	10.62	8.86	−0.1	0.07	−1.74
NNO	*12.9*	12.27	11.12	1.1	0.69	−1.51
$H_2CN(H)CH_2$	6.9	7.31	7.50	−1.4	−0.26	−1.20
$H_2CN(H)NH$	8.6	8.52	7.92	−0.3	−0.20	−1.55
$H_2CN(H)O$	9.7	9.67	9.77	0.5	0.48	−1.05
H_2COCH_2	7.1	7.50	7.72	−0.4	−0.21	−0.41
H_2CONH	8.6	8.75	7.81	0.2	0.21	−0.97
H_2COO	10.3	9.67	9.67	0.9	0.47	−0.34
OOO	*13.5*	12.75	11.28	*2.2*	1.41	1.00

[a] Italic values are experimental photoelectron spectroscopic values. See ref 5. [b] J. Bastide and J. P. Maier, *Chem. Phys. (Utrecht)*, **12**, 177 (1976). [c] T. H. Lee, R. J. Colton, M. G. White, and J. W. Rabalais, *J. Am. Chem. Soc.*, **97**, 4845 (1975).

tronegativity to X, the $X^-{=}Y^+{=}Z$ structure increases in stability relative to the other structure. Bending at the X center causes stabilization because of the increase of s character (hybridization) in the orbital bearing negative charge. Two C=N double bonds are formally retained in the bent geometry. Bending at the Z center also causes stabilization of the lone pair, but here a triple bond is retained.

The sacrifice in allyl resonance appears to be largely compensated for by the stabilization due to hybridization. Moreover, the larger stability of the two cumulated π bonds in $X^-{=}Y^+{=}Z$ in comparison with the less stable alkyne-like combination of π bonds in $X^-{\equiv}Y^+{-}Z$ appears to be a discriminating factor as far as the site of bending is concerned.

A clearer rationalization can be given in orbital terms. Thus, the planar ylide has a very high-lying HOMO which is substantially stabilized upon bending by mixing with vacant σ^* orbitals. An orbital mainly σ^*_{CH} in character is low lying and will overlap well with the HOMO upon bending. Along the series from ylide to oxide the HOMO decreases in energy and becomes more localized at the heteroatom Z, so that bending results in less mixing with the σ^* orbitals.[17] Less bending is found in the series of allyl dipoles, probably as a result of the fact that the needed σ^* orbitals are higher in energy in these cases.

Orbital Energies

In our earlier work, ionization potentials (IP's) and electron affinities (EA's) for parent 1,3-dipoles were estimated.[5] These were obtained from experimental measures in some cases, or were estimated indirectly from other spectroscopic data or calculations. More recently, we have measured photoelectron spectra of a number of nitrones and nitrile oxides.[6] One of the strengths of MINDO methods is the reasonable estimation, using Koopmans' theorem, without correction factors, of IP's and EA's. As shown in Table II, there is good agreement between the negatives of MINDO/2 orbital energies and the ionization potentials and electron affinities estimated earlier. Curiously, MINDO/3, which gives better geometries than MINDO/2, gives poorer IP and EA estimates, particularly for the diazonium betaines for which experimental IP's are available. The EA's in MINDO/3 are uniformly more negative (usually by about 1 eV) than those in MINDO/2.

For the most part, the eigenvectors, π, and total charges are similar to those reported earlier by CNDO/2 method.[5] Rather than tabulate these here, we will make these available to interested readers upon request. However, since the eigenvectors

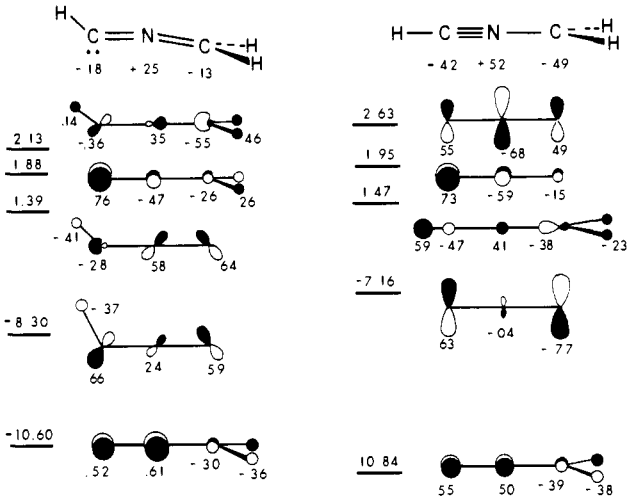

Figure 10. MINDO/3 frontier molecular orbital energies and coefficients for fully optimized and planar-optimized nitrile ylide (numbers below drawings are gross atomic charges).

for bent nitrilium betaines were not reported in our previous paper, we give those for nitrile ylide in Figure 10.

The coefficients of the bent form shown in Figure 10 illustrate the significantly large changes in the FMO's accompanying bending. In the bent ylide (and also the imine), the X carbon becomes the nucleophile center whereas Z is now the electrophilic end of the dipole. The availability of a large coefficient at C on a vacant π^* orbital can explain the recently discovered carbene-like additions of nitrile ylides, imines, and oxides, as discussed earlier.[13] In the oxide the change in electrophilicity characteristics is relatively small and not enough to change our previous conclusions.[5]

Conclusions

The present work shows that the geometries of 1,3-dipoles are significant in determining the types of reactivities these species exhibit. The perturbation treatment reveals the origin of the shapes of the 1,3-dipole MO's and makes a qualitative prediction of substituent effects on frontier orbital energies and coefficients possible.

Both MINDO/2 and MINDO/3 reproduce trends in 1,3-dipole geometries reported earlier by ab initio techniques.[13] While MINDO/2 seems to give more reliable IP's and EA's, MINDO/3 gives significantly better geometries. Thus, these semiempirical methods, which are generally suspect for mol-

ecules containing adjacent atoms with lone pairs, turn out to give some reasonably accurate predictions.

Acknowledgment. The authors are grateful to the National Science Foundation and the National Institutes of Health for partial financial support of this research and to Robert W. Strozier and Alex Nicolson for modifications of the computer programs used in this work.

References and Notes

(1) (a) NATO Fellow, 1975; on leave from the University of Pavia, Italy; (b) Camille and Henry Dreyfus Foundation Teacher-Scholar Grant Recipient, 1972–1977; Alfred P. Sloan Foundation Fellow, 1975–1977.
(2) R. Huisgen, *Angew. Chem., Int. Ed. Engl.*, **2**, 565, 633 (1963).
(3) R. Sustmann, *Tetrahedron Lett.*, 2717 (1971).
(4) K. N. Houk, *J. Am. Chem. Soc.*, **94**, 8953 (1972); K. N. Houk, J. Sims, C. R. Watts, and L. J. Luskus, *ibid.*, **95**, 7301 (1973).
(5) K. N. Houk, J. Sims, R. E. Duke, Jr., R. W. Strozier, and J. K. George, *J. Am. Chem. Soc.*, **95**, 7287 (1973).
(6) J. Bastide and O. Henri-Rousseau, *Bull. Soc. Chim. Fr.*, 2294 (1973); J. Bastide, N. El Ghandour, and O. Henri-Rousseau, *ibid.*, 2290 (1973).
(7) A. Komornicki and J. W. McIver, Jr., OPTMO, Quantum Chemistry Program Exchange, No. 217; J. W. McIver, Jr., and A. Komornicki, *Chem. Phys. Lett.*, **10**, 303 (1971).
(8) N. Bodor, M. J. S. Dewar, E. Haselbach, and A. Harget, *J. Am. Chem. Soc.*, **92**, 3854 (1970).
(9) M. J. S. Dewar, H. Metiu, P. J. Student, A. Brown, R. C. Bingham, D. H. Lo, C. A. Ramsden, H. Kollmar, P. Weiner, and P. K. Bischof, MINDO/3, Quantum Chemistry Program Exchange, No. 279; R. C. Bingham, M. J. S. Dewar, and D. H. Lo, *J. Am. Chem. Soc.*, **97**, 1285, 1294, 1302, 1307 (1975).
(10) See, for example, M. J. S. Dewar, "The Molecular Orbital Theory of Organic Chemistry", McGraw-Hill, New York, N.Y., 1973; L. Libit and R. Hoffmann, *J. Am. Chem. Soc.*, **96**, 1370 (1974).
(11) A. Imamura and T. Hirano, *J. Am. Chem. Soc.*, **97**, 4192 (1975).
(12) Calculations were carried out by setting matrix elements corresponding to $2p_z$–$2p_z$ interactions equal to 0: H. L. Hase and A. Schweig, *Tetrahedron*, **29**, 1759 (1973).
(13) P. Caramella and K. N. Houk, *J. Am. Chem. Soc.*, **98**, 6397 (1976).
(14) E. F. Hayes and A. K. Q. Siu, *J. Am. Chem. Soc.*, **93**, 2090 (1971).
(15) A. J. Arduengo and E. M. Burgess, *J. Am. Chem. Soc.*, **98**, 5021 (1976).
(16) K. N. Houk, P. Caramella, L. L. Munchausen, Y.-M. Chang, A. Battaglia, J. Sims, and D. C. Kaufman, *J. Electron Spectrosc. Relat. Phenom.*, in press.
(17) This type of reasoning was proposed for AH_3 molecules by C. C. Levin, *J. Am. Chem. Soc.*, **97**, 5649 (1975).
(18) NOTE ADDED IN PROOF. Optimizations by 4-31G give the following HCN angles for nitrilium betaines: ylide, 123°; imine, 180°; oxide, 180°.
(19) A planar geometry with a COC angle of 129° has been found from an STO-3G optimization: G. Leroy, M.-T. Nguyen, and M. Sana, *Tetrahedron*, **32**, 1529 (1976).

Thermal Sigmatropic [1,*j*] Shifts in Cyclic Systems. A Perturbation Approach and INDO Calculations

Jan R. de Dobbelaere,* Jan M. F. van Dijk, Jan W. de Haan, and Henk M. Buck

Contribution from the Department of Organic Chemistry, Eindhoven University of Technology, The Netherlands. *Received April 27, 1976*

Abstract: Some fundamental aspects of sigmatropic shifts are discussed with the help of INDO calculations and perturbation theory. In cyclic systems the degeneracy of the highest occupied molecular orbital is lifted in the transition state. A suprafacial H shift is determined by a combination of the 1s orbital of the migrating hydrogen with the symmetric MO's of the system and an antarafacial shift by a combination with the antisymmetric MO's. The used perturbation model offers the possibility to reconcile somewhat the concepts of "allowed" and "forbidden". Formally forbidden reactions which, however, have been found experimentally can be explained with this model. Many "forbidden" reactions are in fact "allowed", but they proceed with a higher activation enthalpy. Some transition state geometries have been calculated and the occurring charge transfer is explained in terms of aromaticity.

In 1965 Woodward and Hoffmann postulated their concept of orbital symmetry rules governing pericyclic reactions.[1] In the particular case of sigmatropic reactions, the transition state is thought to be determined by the migrating group and the HOMO or LUMO of the radical-like species left behind, after splitting off the migrating group in thermal and photochemical rearrangements, respectively. In principle, the symmetry properties of the HOMO or LUMO were considered for acyclic polyenes. The major part of the experimental work reported in the last ten years is in agreement with the predictions.

Curiously enough, this applied also to a host of cyclic systems. Whereas the description of acyclic systems is relatively straightforward, cyclic systems have, so far, defied a truly general explanation. The major problem has been the fact that in these systems all but the lowest molecular orbitals are doubly degenerate in the transition state. In 1968 Anastassiou tried to work out the degeneracy problem in C_nH_{n+1} monocycles.[2] It was postulated that the presence of the migrating group will disturb the symmetry of the radical, thereby lifting the degeneracy. It was then concluded that the migrating group will combine with the "genuine" HOMO again.

In our opinion, however, the real perturbation is formed by a hydrogen nucleus *in the transition state* in contrast with Anastassiou's approach in which the perturbation was applied to the reactant. This leads to an entirely different result (see also next section).

There are no compelling reasons to confine the discussion to the HOMO, as already suggested by Berson[3] and, in a more elaborate way, by Anh[4] and Fukui,[5] who worked out the application of perturbation theory to pericyclic rearrangements. The implications of this method have, so far, not been discussed in detail for sigmatropic rearrangements. In general, the nomenclature and selection rules derived for acyclic systems are used without modifications for cyclic polyenes as well.

Here we wish to present evidence that simple perturbation theory allows one to predict several aspects of [1,*j*] rearrangements in simple systems in a relatively simple fashion. The results are substantiated by INDO calculations. Before specific examples are discussed, it should be realized that a migrating hydrogen, involved in a suprafacial shift, will have to interact with symmetric molecular orbitals. On the other hand, in antarafacial rearrangements the interaction necessarily originates from combination with asymmetric orbitals.